Available online at www.sciencedirect.com
SCIENCE DIRECT®
Journal of Solid State Chemistry 177 (2004) 2610–2616
JOURNAL OF SOLID STATE CHEMISTRY
http://elsevier.com/locate/jssc

Crystal structure and energy band and optical properties of phosphate $Sr_3P_4O_{13}$

Y.-C. Zhang, W.-D. Cheng,* D.-S. Wu, H. Zhang, D.-G. Chen, Y.-J. Gong, and Z.-G. Kan

State Key Laboratory of Structural Chemistry, The Graduate School of the Chinese Academy of Sciences, Fujian Institute of Research on the Structure of Matter, Fuzhou, Fujian 350002, China

Received 25 November 2003; received in revised form 18 February 2004; accepted 10 March 2004

Abstract

A single crystal of the compound $Sr_3P_4O_{13}$ has been found and the crystal structure has been characterized by means of single crystal X-ray diffraction analysis. The compound crystallizes in triclinic system and belongs to space group $P\bar{1}$. It builds up from SrO_7 polyhedra and $P_4O_{13}^{-6}$ anions and has a layered structure, and the Sr atoms are located in the interlayer space. The absorption and luminescence spectrum of $Sr_3P_4O_{13}$ microcrystals have been measured. The calculated results of crystal energy band structure by the DFT show that the solid state of $Sr_3P_4O_{13}$ is an isolator with direct band gap. The calculated total and partial density of states indicate that the top valence bands are contributions from P 3*p* and O 2*p* states and low conduction bands mostly originate from Sr atomic states. The calculated optical response functions expect that the $Sr_3P_4O_{13}$ is a low refractive index, and it is possible that the $Sr_3P_4O_{13}$ is used to make transparent material between the UV and FR light zone.

Keywords: Crystal structure; Energy band; Optics properties; Phosphate

1. Introduction

Divalent phosphates, such as $M_3(PO_4)$ with $M = Mg^{2+}$, Ca^{2+}, Sr^{2+}, Cd^{2+}, Zn^{2+}, have been studied during the past years for their luminescent applications [1–4]. Koelmans and Cox [1] investigated the luminescence characteristics of tin-activated strontium orthophosphate containing various amounts of Ca^{2+}, Mg^{2+}, Zn^{2+}, Cd^{2+}, or Al^{3+}. Introduction of these ions into $Sr_3(PO_4)_2$ led to the formation of a material isotypic with β-$Ca_3(PO_4)_2$ and different from the usually observed structure of $Sr_3(PO_4)_2$. Levshin et al. [5] also described the luminescence of Eu^{2+}-activated $Sr_3(PO_4)_2$. Some alkaline earth halophosphates, such as $3Ca_3(PO_4)_2{\cdot}CaF_2$, have been used in most phosphors for fluorescent lights [6]. In general, these orthophosphates show polymorphic transitions and their luminescence properties are dependent on the polymorph [4]. Additionally, study of optical absorption in the gel-grown $BaHPO_4$ crystals in UV-VIS range revealed transitions assisted by absorption and emission of phonons [7]. When we search for a new optical material in phosphates, a new crystal $Sr_3P_4O_{13}$ was found. As we know, phosphates are important phosphor hosts, such as divalent tin-activated β-$Sr_3(PO_4)_2$ and divalent manganese-activated β-$Zn_3(PO_4)_2$, which have been used as a color corrector in high-pressure mercury vapor lamps and as the red component in color television screens, respectively. Phosphates are also important nonlinear optical materials, such as $KTiOPO_4$ and $NH_4H_2PO_4$, which have been used to frequency conversion and laser spectrum. McKeag and Steward [8] published an X-ray diffraction pattern for a sample of $Sr_3P_4O_{13}$ containing 2% tin, and Kriedler and Hummel [9] gave a more complete X-ray diffractometer pattern for the pure material of the $Sr_3P_4O_{13}$ (strontium tetraphosphate). In this work, we will present the synthesis, crystal structure determination, and spectrum measurements, as well as the calculations of crystal energy band structures and optical response functions of $Sr_3P_4O_{13}$ species.

*Corresponding author. Laboratory of Chemistry and Physics of Materials, Fujian Institute of Research on the Structure of Matter, Yang Qiao Xi Road No. 155, Fuzhou, Fujian 350002, China. Fax: +86-591-371-4946.

E-mail address: cwd@ms.fjirsm.ac.cn (W.-D. Cheng).

0022-4596/$ - see front matter © 2004 Elsevier Inc. All rights reserved.
doi:10.1016/j.jssc.2004.03.029

2. Experimental and computional procedures

2.1. Synthesis

Single crystals of $Sr_3P_4O_{13}$ were grown by melting a mixture of analytical grade Li_2CO_3, $SrCO_3$ and $NH_4H_2PO_4$, in the molar ratio: 2:3:6. After grinding in agate mortar, the mixture was put into a platinum crucible and heated to 573 K and kept at this temperature for 4 h to decompose the $NH_4H_2PO_4$, followed by heating at 1003 K for 10 h, then cooled from 1003 to 873 K at a rate of $5\,K/h^{-1}$ and finally air-quenched to room temperature. The crystals obtained are sheet and colorless.

2.2. X-ray single crystal structure determination

A crystal of approximate dimensions $0.30 \times 0.24 \times 0.22\,mm^3$ was selected carefully. The diffraction data were collected on a Siemens SMART CCD diffractometer with graphite monochromated Mo$K\alpha$ radiation ($\lambda = 0.71073$ Å) at the temperature of 293 K using the $\omega/2\theta$ scan mode. Unit-cell parameters were determined by least-squares refinement of 2829 reflections, affording 1782 unique reflections with $R_0^2 \geqslant 2\sigma(F_0^2)$. Lorentz and polarization corrections were applied to the data.

The crystal structure was determined with the SHELXL software. The positions of the Sr atoms were located by application of the direct methods with SHELXL program; the remaining atoms were located in succeeding difference Fourier synthesis. Further details of the X-ray structural analysis are give in Table 1. The atomic coordinates and thermal parameters are listed in Table 2. Selected bond lengths and angles are given in Table 3.

2.3. Spectrum measurement

The samples used for spectrum measurement were prepared from pressed abradant of selected single-crystals. For these processes, we firstly pick out several single-crystals and determinate the unit cell parameters of these single-crystals in order to obtain pure $Sr_3P_4O_{13}$ phase, then we put the single crystals together and grind them. The absorption spectrum was recorded by a Perkin-Elmer Lambda 900 UV/Vis/NIR spectrophotometer in the wavelength range of 200–800 nm and the luminescence is measured by Edinburgh Instrument F920 fluorescent spectrometer using Xe lamp at room temperature.

2.4. Computational descriptions

The crystallographic data of phosphate oxide $Sr_3P_4O_{13}$ determined by X-ray was used to calculate

Table 1
Crystallographic data for the title compound

Empirical formula	$Sr_3P_4O_{13}$
Formula weight	594.74
T (K)	293(2)
Wavelength (Å)	0.71073
Crystal system	Triclinic
Space group	$P\bar{1}$
A (Å)	7.2755(1)
b (Å)	7.7260(1)
c (Å)	10.1935(2)
α (°)	102.28(0)
β (°)	103.46(0)
γ (°)	94.35(0)
V (Å^3)	537.75(16)
Z	2
Calculated density (g/cm^3)	3.659
Absorption coefficient (mm^{-1})	15.44
$F(000)$	556.0
Crystal size (mm)	$0.30 \times 0.24 \times 0.22$
θ range for data collection (°)	2.11–25.06
Index ranges	$-8 \leqslant h \leqslant 8$, $-9 \leqslant k \leqslant 5$, $-12 \leqslant l \leqslant 12$
Reflections collected	2829
Reflections unique	1782 ($R_{int} = 0.0410$)
Completeness to $\theta = 25.06$	93.1%
Refinement method	Full-matrix least-squares on F^2
Data/restraints/parameters	2829/0/182
Goodness-of-fit on F^2	1.046
Final R indices [$I > 2\sigma(I)$]	$R_1 = 0.0488$ $\omega R_2 = 0.1169$
R indices (all data)	$R_1 = 0.0668$ $\omega R_2 = 0.1304$
Largest difference peak and hole (e/A^3)	1.126 and −0.931

Table 2
Fractional atomic coordinates and equivalent isotropic displacement parameters (Å^2) for the title compound

Atom	x	y	z	U_{eq}[a]
Sr1	0.24861(11)	0.98443(11)	0.24312(8)	0.0096(3)
Sr2	0.29161(12)	0.78097(11)	−0.13614(8)	0.0077(3)
Sr3	0.21542(12)	1.22782(11)	0.62632(8)	0.0086(3)
P1	0.3627(3)	0.5397(3)	0.1418(2)	0.0063(5)
P2	0.3287(3)	0.8092(3)	0.5129(2)	0.0062(5)
P3	0.1746(3)	1.1909(3)	−0.0214(2)	0.0057(5)
P4	−0.1374(3)	0.5373(3)	−0.3474(2)	0.0058(5)
O1	0.3366(8)	1.1000(8)	0.0466(6)	0.0085(13)
O2	0.1551(9)	0.8966(8)	0.4551(6)	0.0102(13)
O3	0.1187(9)	1.1196(8)	−0.1786(6)	0.0114(14)
O4	0.2633(9)	0.3985(7)	0.0004(6)	0.0082(13)
O5	0.3975(9)	0.8718(8)	0.6670(6)	0.0127(14)
O6	0.3691(9)	0.7179(8)	0.1096(6)	0.0129(14)
O7	0.4742(9)	0.8186(8)	0.4300(6)	0.0134(14)
O8	0.0657(9)	0.5124(8)	−0.3173(6)	0.0130(14)
O9	0.2542(9)	0.5980(8)	0.4867(6)	0.0114(14)
O10	0.0100(10)	1.1924(9)	0.0439(7)	0.0209(16)
O11	−0.1812(10)	0.7178(9)	−0.3636(7)	0.0180(15)
O12	0.2092(9)	0.5323(9)	0.2303(6)	0.0175(15)
O13	0.5450(9)	0.4899(9)	0.2125(6)	0.0147(15)

[a] $U_{eq} = \frac{1}{3}\sum_i \sum_j U^{ij} \alpha_i * \alpha_j * a_i a_j$.

Table 3
Selected bond lengths (Å) and bond angles (°) for the title compound

Atoms	Distances	Atoms	Distances
Sr1–O11i	2.507(8)	Sr3–O2viii	2.667(7)
Sr1–O1	2.548(7)	Sr3–O2	2.715(7)
Sr1–O6	2.548(7)	Sr3–O11i	2.757(8)
Sr1–O5ii	2.596(7)	Sr3–O5	3.206(7)
Sr1–O2	2.613(7)	P1–O13	1.477(7)
Sr1–O3i	2.619(7)	P1–O6	1.480(7)
Sr1–O7	2.802(8)	P1–O4	1.586(6)
Sr1–O10i	3.051(8)	P1–O12	1.595(8)
Sr1–O10	3.144(9)	P2–O5	1.494(6)
Sr2–O5iii	2.518(7)	P2–O7	1.508(8)
Sr2–O13iv	2.552(8)	P2–O2	1.531(7)
Sr2–O10i	2.586(8)	P2–O9	1.626(7)
Sr2–O6	2.597(7)	P3–O10	1.500(8)
Sr2–O8	2.619(8)	P3–O1	1.521(7)
Sr2–O1v	2.667(6)	P3–O3	1.523(6)
Sr2–O1	2.701(8)	P3–O4ix	1.632(7)
Sr2–O3	3.055(7)	P4–O8	1.474(7)
Sr3–O7ii	2.489(7)	P4–O11	1.489(8)
Sr3–O3vi	2.535(7)	P4–O9x	1.580(6)
Sr3–O8vii	2.543(7)	P4–O12x	1.584(8)
Sr3–O13ii	2.656(8)		

Atoms	Angle	Atoms	Angle
O13–P1–O6	116.70(39)	O1–P3–O3	110.88(34)
O13–P1–O4	111.98(35)	O10–P3–O4ix	107.31(38)
O6–P1–O4	106.85(35)	O1–P3–O4ix	106.13(35)
O13–P1–O12	111.01(39)	O3–P3–O4ix	103.79(34)
O6–P1–O12	106.53(37)	O8–P4–O11	116.24(41)
O4–P1–O12	102.70(33)	O8–P4–O9x	110.75(36)
O5–P2–O7	117.36(35)	O11–P4–O9x	105.88(38)
O5–P2–O2	111.77(35)	O8–P4–O12x	103.33(38)
O7–P2–O2	110.43(38)	O11–P4–O12x	116.22(39)
O5–P2–O9	104.28(34)	O9x–P4–O12x	103.81(32)
O7–P2–O9	105.63(36)	P1–O4–P3xii	128.37(51)
O2–P2–O9	106.41(35)	P4x–O9–P2	128.69(56)
O10–P3–O1	113.60(39)	P4x–O12–P1	150.5(6)
O10–P3–O3	114.23(37)		

Symmetry codes: (i) $-x, 2-y, -z$; (ii) $1-x, 2-y, 1-z$; (iii) $x, y, -1+z$; (iv) $1-x, 1-y, -z$; (v) $1-x, 2-y, -z$; (vi) $x, y, 1+z$; (vii) $x, 1+y, 1+z$; (viii) $-x, 2-y, 1-z$; (ix) $x, 1+y, z$; (x) $-x, 1-y, -z$; (xi) $x, -1+y, -1+z$; (xii) $x, -1+y, z$.

electronic band structures of the solid state. The calculations of band structures were made by the density functional theory (DFT) with local gradient-corrected exchange-correlation functional (LDA) [10] and performed with the CASTEP code [11,12], which uses a plane wave basis set for the valence electrons and norm-conserving pseudopotential [13] for the core states. The number of plane waves included in the basis was determined by a cutoff energy E_c. Pseudoatomic calculations were performed for O $2s^2 2p^4$, P $3s^2 3p^3$, Sr $4s^2 4p^6 5s^2$. The calculating parameters and convergent criterions were set by the default values of CASTEP code [11]. The calculations of linear optical properties were also made in this work. The imaginary part of the dielectric function, $\varepsilon(\omega)_2$, is given by equation CASTEP 64 [11], and $\varepsilon(\omega)_2$ can be thought of as detailing the real transitions between occupied and unoccupied electronic states. Since the dielectric constant describes a causal response, the real and imaginary parts are linked by a Kramers–Kronig transform. This transform is used to obtain the real part of the dielectric function, $\varepsilon(\omega)_1$.

3. Results and discussions

3.1. Crystal structure

Single crystal X-ray diffraction analysis shown that the $Sr_3P_4O_{13}$ compound crystallizes in triclinic system, space group $P\bar{1}$, with $a = 7.2755(1)$, $b = 7.7260(1)$, $c = 10.1935(2)$ Å, $\alpha = 102.28(0)°$, $\beta = 103.46(0)°$, $\gamma = 94.35(0)°$, $V = 537.75(16)$ Å^3, $Z = 2$, $R_1 = 0.0488$. This compound has a layered structure, which contains SrO_7 polyhedra and tetrapolyphosphate $P_4O_{13}^{-6}$ anions (Fig. 1). Fig. 2 gives a perspective view of the $Sr_3P_4O_{13}$ molecule. The $(P_4O_{13}^{-6})_n$ infinite layers are built up from P_4O_{13} that are composed of four PO_4 tetrahedrons. The Sr atoms are located in the interlayer space. Two chemically and crystallographically distinct P atoms are present in the structure: P1 (P4) and P2 (P3). In case of P(1)O4 tetrahedron, O4 and O12 are shared by two P atoms, respectively, and the average distance of P(1)–O4 and P(1)–O12 is 1.591 Å, whereas the average distance of P(1)–O6 and P(1)–O13, for which the O6 and O13 are shared by P(1), respectively, is significantly shorter: 1.479 Å. For P(2) atom, it connects with O2, O5, and O7 atoms and their average distance is 1.510 Å, but P(2)–O9 {O9 connected with P(2) and P(4)} distance is much longer: 1.619 Å. The O–P–O angles range from 102.70° to 117.36°, whereas the P–O–P bridge angles of the O–P–O–P–O–P–O–P–O chains are about 128.5° and 150.5° (Table 3). The torsional angles of P(3)–O(4)–P(1)–O(12) and P(1)–O(12)–P(4)–O(9) are –52.89° and 83.11°, as

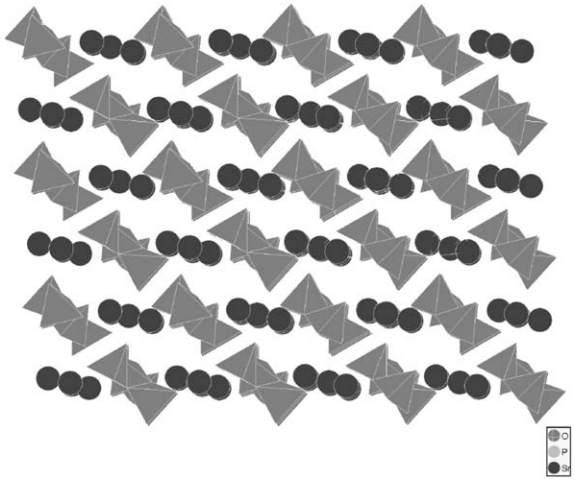

Fig. 1. Projection of the structure of $Sr_3P_4O_{13}$ along [011]. Solid circles: Sr.

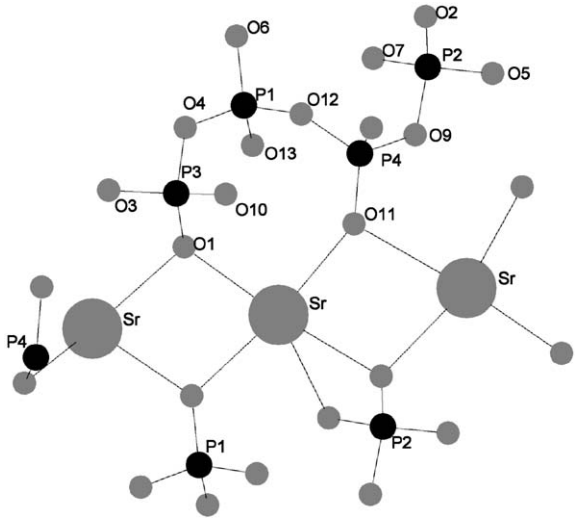

Fig. 2. The perspective view of $Sr_3P_4O_{13}$, the *a*-axis is approximately perpendicular to this plane.

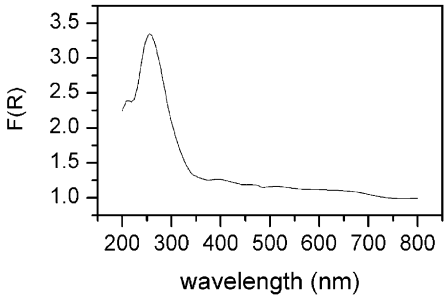

Fig. 3. Absorption spectrum of $Sr_3P_4O_{13}$ in little solid crystals.

shown in Fig. 2, respectively. The coordination numbers of Sr atoms were determined on the basis of the maximum gap in the Sr–O distances ranked in increasing order. All the Sr atoms are therefore coordinated by 7 oxygen atoms with the 8th Sr(1)–O10i, 9th Sr(1)–O10, 8th Sr(2)–O3, and 8th Sr(3)–O5 distances at 3.051(8), 3.144(9), 3.055(7), and 3.20(7) Å, individually. The Sr–O bond length range is 2.489(7)–2.802(8) Å, comparing closely to the range {2.468(8)–2.805(9) Å} observed in SrO_7 polyhedra [14].

3.2. Spectrum properties

Fig. 3 shows the absorption spectrum of $Sr_3P_4O_{13}$. From this figure we can see a sharp absorption peak at 250 nm and a wide transmission range from 330 to 800 nm. A broad emission spectrum from 450 to 505 nm (as shown in Fig. 4) was obtained when a light of 251 nm excited this crystal. The strongest emission peak is located at 470 nm. The observed absorption cut off edge is at about 330 nm (3.76 eV) shown in Fig. 3 as compared with the observed emitted peak localized at about 470 nm (2.64 eV) shown in Fig. 4, we can deduce that the emitted fluorescence of $Sr_3P_4O_{13}$ originates from defects or excitons due to emission energy of 2.64 eV is less than the optical absorption edge of 3.76 eV.

3.3. Band structure and density of states

The calculated band structures of phosphate oxide $Sr_3P_4O_{13}$ at the Brillouin zone is shown in Fig. 5. It is observed whether the conduction bands or valence bands are flat, and this solid state shows an isolator and the direct band gap at about 4.76 eV. The bands lying about −32 eV and about −14 eV are contributions from the Sr 4*s* and 4*p* states, respectively. The valence bands localized between −16 and −22 eV are most contributions from O 2*s* states, but mixing with a little P 3*s* and 3*p* states. The valence bands between −5.6 eV

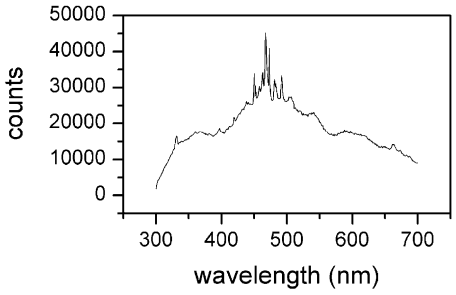

Fig. 4. Luminescence spectrum of $Sr_3P_4O_{13}$ in little solid crystals (excited at 251 nm).

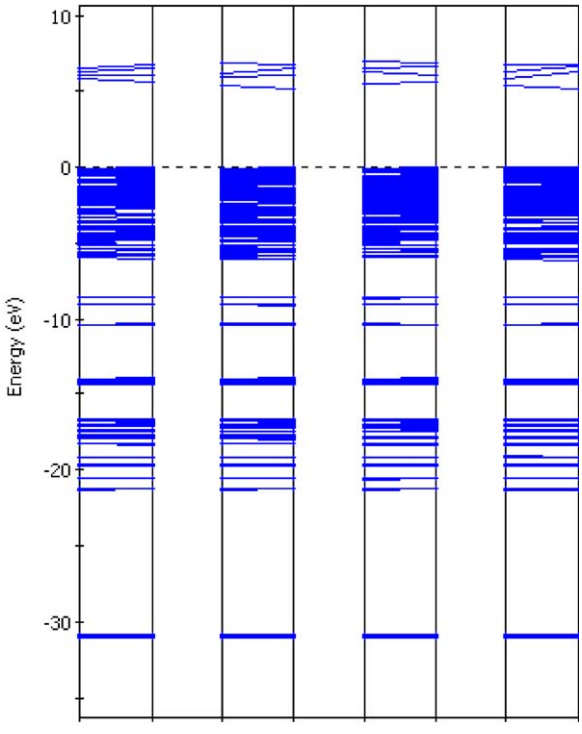

Fig. 5. Electronic band structure of $Sr_3P_4O_{13}$.

and the Fermi level (0.0 eV) are crowed and formed by the O 2*p* and P 3*p* states, mixing with a small P 3*s* states. The highest level at the valence bands is almost contribution from the O 2*p* states. The lowest conduction bands are mainly due to Sr 5*s* states hybridized with small P 3*s* and 3*p* states. Accordingly, the absorption peak of electronic spectrum of pressed abradant of microcrystal $Sr_3P_4O_{13}$ that is observed at 250 nm (4.96 eV), as shown in Fig. 3, is assigned as the charge transfers from the O 2*p* to Sr^{2+} 5*s* states. The calculated band gap of 4.76 eV is as compared with the experimental absorption edge of 3.76 eV. Generally, the LDA method underestimates the gap energy and the scissor operator (shift energy) technique corrects this discrepancy [11,12]. The calculated direct gap of 4.76 eV between the conduction and valence bands of $Sr_3P_4O_{13}$ crystal is larger than the direct band transition gap (2.38–3.26 eV) of $BaHPO_4$ crystal assisted by lattice phonons [7]. It takes larger energies for the photon transition than the lattice phonon transition that seems reasonable.

Further, we have also calculated the total, atomic site and angular momentum projected densities of states (DOS) of $Sr_3P_4O_{13}$, as displayed in Figs. 6 and 7, respectively, in order to elucidate the nature of the electronic band structures. Comparing the total DOS with the angular momentum projected DOS of $Sr_3P_4O_{13}$ for P 3*p* and O 2*p* states displayed in Fig. 6, we can find that from −5.6 to 0.0 eV, even though the DOS for O 2*p* is higher than that of P 3*p*, they are fairly closed. This shows that some electrons from P 3*p* transform into the valence bands and take part in the interactions between P and O atoms. This case tells us that there are hybridization between P 3*p* and O 2*p* states and covalence bond characters between P and O atoms. It is also evident from the population analysis. The calculated bond orders between P and O atoms in a unit cell are from 0.40 to 0.80e, in which the bond order is between 0.50 and 0.80e for 22 P–O bonds and between 0.40 and 0.50e for 8 P–O bonds (the covalence single bond order is general 1.0e). On the other hand, comparing the total DOS with the site projected DOS of Sr, it is found that the peaks of total DOS around −32 eV and around −14 eV completely attribute to Sr 4*s* and 4*p* states. This implies that there is ionic bond character between Sr and O atoms. The calculated bond orders between Sr and O atoms are below 0.10e and the lowest bond order is 0.05e between Sr and O atoms.

3.4. Optical properties

Now, we examine the linear optical response properties. The calculated imaginary part $\varepsilon_2(\omega)$ and the real $\varepsilon_1(\omega)$ part of the frequency-dependent dielectric function without the DFT scissor-operator approximation are displayed in Fig. 8. The part $\varepsilon_2(\omega)$ can be used to describe the real transitions between occupied and unoccupied electronic states. It is found from the dispersion of the calculated $\varepsilon_2(\omega)$ spectra that there is a wide transparent from wavelengths of 300–1200 nm and an absorption band localized about 160 nm for phosphate crystal $Sr_3P_4O_{13}$. The calculated dielectric constant of static case, $\varepsilon(0)$ [$\varepsilon(0) \approx \varepsilon_1(0)$ at low frequency], is about 1.62. The frequency-dependent refractive index are also calculated by the relation of $n^2 = \varepsilon$, and the static refractive index of n_x, n_y, n_z is 1.27,

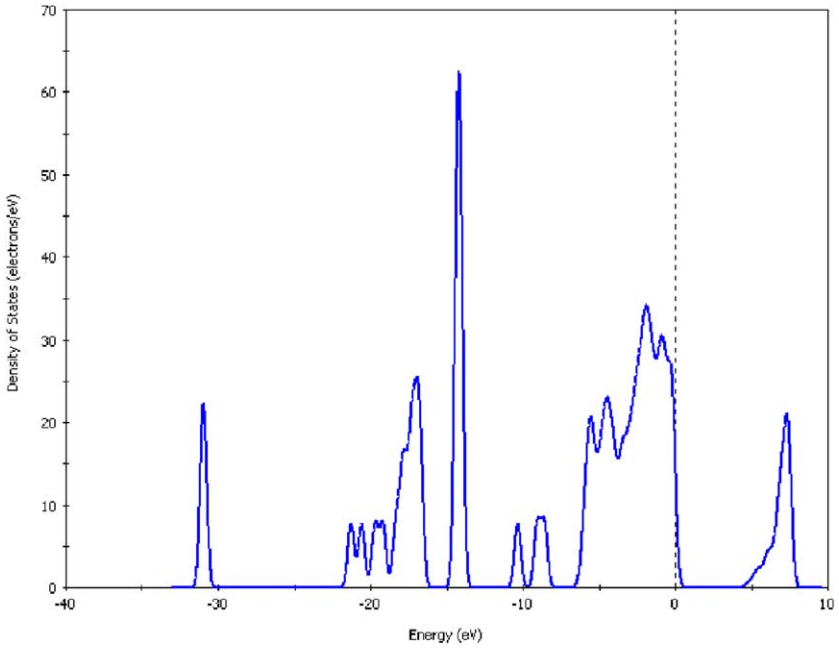

Fig. 6. The total density of state of phosphate oxide $Sr_3P_4O_{13}$ based on DFT calculations.

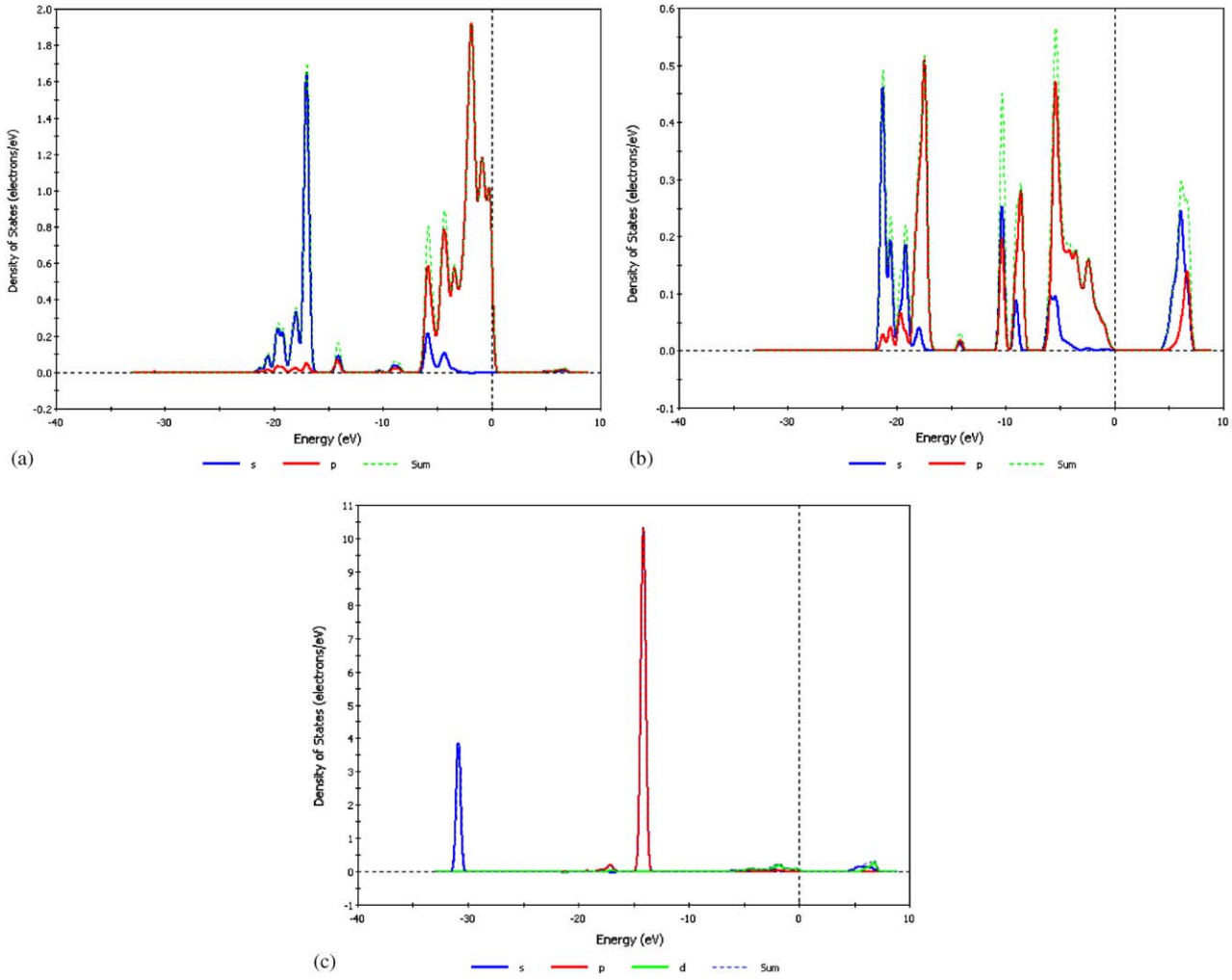

Fig. 7. (a) The partial density of state for O in $Sr_3P_4O_{13}$ based on DFT calculations. (b) The partial density of state for P in $Sr_3P_4O_{13}$ based on DFT calculations. (c) The partial density of state for Sr in $Sr_3P_4O_{13}$ based on DFT calculations.

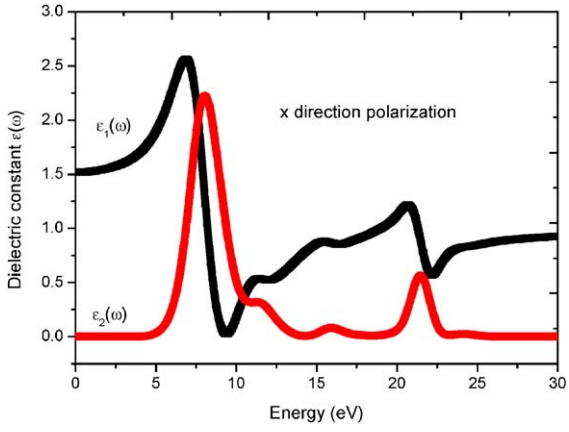

Fig. 8. The calculated dielectric constants of $Sr_3P_4O_{13}$ crystal.

1.28, and 1.26, individually. It is reported that the observed refractive index of phosphate is generally ranging from 1.40 to 1.60. For example, the refractive index of $Ca(PO_3)_2$ and $Ca_2P_2O_7$ are 1.588 and 1.585, respectively [15]. Comparing with the observed refractive index of the other phosphate crystals, our calculated refractive index of the phosphate crystal $Sr_3P_4O_{13}$ at static case may be underestimate about 10–20%.

4. Conclusions

In the present work, a single-crystal structure of $Sr_3P_4O_{13}$ compound has been determined and it crystallizes in triclinic system with space group $P\bar{1}$. Observe the absorption peak it is at about 250 nm and emitted peak is at about 470 nm for the power phase. The calculated band structures shows that the solid state of $Sr_3P_4O_{13}$ is an isolator with direct band gap at about 4.76 eV and the optical transition of lowest energy mainly originates from O $2p$ to Sr^{2+} $5s$ states. In the $Sr_3P_4O_{13}$, the PO_4 tetrahedrons are covalence bond characters and the SrO_7 polyhedrons are ionic bond characters. The optical

dielectric constant of the crystal is estimated to be 1.62 taking as theoretical prediction.

Acknowledgments

This investigation was supported by the National Science Foundation of China (No. 90201015), the Science Foundation of the Fujian Province (No. E0210028, and No. 2002F010), and the Foundation of State Key Laboratory of Structural Chemistry (No. 030060).

References

[1] H. Koelmans, A.P.M. Cox, J. Electrochem. Soc. 104 (1957) 442–445.
[2] J.F. Sarver, M.V. Hoffman, F.A. Hummel, J. Electrochem. Soc. 108 (1961) 1103–1110.
[3] E.R. Kreidler, F.A. Hummel, Inorg. Chem. 6 (1967) 524–528.
[4] J.R. Looney, J.J. Brown, J. Electrochem. Soc. 118 (1971) 470–473.
[5] V.L. Levshin, et al., Trans. P.N. Lebedev, Physics Inst. "Soviet Research on Luminescence," in: D.V. Skabel'tsyn (Ed.), (English Transl.), Consultants Bureau, New York, 1964 (Chapter 3).
[6] L. Smart, E. Moore, Solid State Chemistry, An Introduction, Chapman & Hall, London, 1992, pp. 220.
[7] S.K. Arora, T.R. Trivedi, V.A. Patel, Scr. Mater. 47 (2002) 643–647.
[8] A.H. Mckeag, B.G. Steward, Br. J. Appl. Phys. 4 (1955) S26.
[9] E.R. Kreidler, F.A. Hummel, Inorg. Chem. 6 (1967) 884–891.
[10] J.P. Perdew, K. Burke, M. Ernzerhof, Phys. Rev. Lett. 77 (1996) 3865–3868.
[11] M. Segall, P. Lindan, M. Probert, C. Pickard, P. Hasnip, S. Clark, M. Payne, Materials Studio CASTEP version 2.2, 2002.
[12] M.D. Segall, P.L.D. Lindan, M.J. Probert, C.J. Pickard, P.J. Hasnip, S.J. Clark, M.C. Payne, J. Phys.: Condens. Mater. 14 (2002) 2717–2744.
[13] D.R. Hamann, M. Schluter, C. Chiang, Phys. Rev. Lett. 43 (1979) 1494–1497.
[14] K.I. Schaffers, D.A. Keszler, Acta Crystallogr. C 49 (1993) 211–214.
[15] J.A. Dean (Ed.), Lange's Handbook of Chemistry, 13th Edition, McGraw-Hill Book Company, New York, 1985.